



Telomerase-triggered DNzyme spiders for exponential amplified assay of cancer cells



Jing-Lin He*, Yang Zhang, Ting-Ting Mei, Ling Tang, Si-Ying Huang, Zhong Cao**

Hunan Provincial Key Laboratory of Materials Protection for Electric Power and Transportation, School of Chemistry and Food Engineering, Changsha University of Science and Technology, Changsha, 410114, PR China

ARTICLE INFO

Keywords:

DNA walker
Proximity ligation assay
Telomerase
Exponential amplified assay

ABSTRACT

A highly flexible electrochemical assay based on target-triggered DNzyme spiders was proposed for the detection of telomerase. The DNzyme-telomerase substrate primers (D-TSP) containing Cu^{2+} -dependent DNzymes serve as recognition elements, and primers of telomerase. Telomerase extracted from HeLa cells recognize the D-TSP and elongated with DNA sequence repeats. A synthetic telomerase product hybridized with scaffold sequences of two DNzyme-tethered probes on the basis of the mechanism of the proximity-ligation assay. The three-leg DNzyme spiders has been assembled and initiated the autonomous hybridization/nicking/displacement cycles on substrate modified surface. The cleaved ferrocene-labeled fragments are adsorbed on gold surface leading to an increase in the electrochemical signal. As a result, the one input target, telomerase, release large amount of ferrocene-labeled DNA strands, achieving an exponential signal amplification and an excellent improvement in sensitivity over single molecule or two-component 'sandwich' binding complexes. Our proposed biosensor showed a nonlinear dependence with HeLa cell numbers, ranging from 25 to 2000 with a detection limit of 10 cells. Telomerase activities from different cell lines were also successfully evaluated. Our electrochemical strategy based on target-triggered DNzyme spiders was enzyme-free, PCR-free, simple in operation which indicated that it expected to expand the scope of DNA nanotechnology in the areas of clinical diagnosis.

1. Introduction

A DNA machine contains a recognition fragment for its target and a hybridized fragment that connects portions of the strands (Zhang and Winfree, 2009). Some DNA machines were reported, such as tweezers (Li et al., 2016a; Zhang et al., 2017), walkers (Wang et al., 2017; Xu et al., 2017; He et al., 2017), motors (Tomov et al., 2013; Wang et al., 2019) and gears (Nie et al., 2017). DNA walkers are DNA machines that a nucleic acid "walker" autonomously moves along a nucleic acid "track" (Yan et al., 2018). The moving principle integrates cleavage sites and strand displacement strategies to fuel the motion of the walking system. DNzyme was designed to activate DNA walkers in virtue of its cleavage of a ribonucleotide phosphodiester bond through a transesterification reaction (Lund et al., 2010). DNzyme walkers with the autonomous locomotion and remarkable controllability have potential applications in developing biosensors (Qing et al., 2018), diagnostic systems (Li et al., 2018), drug delivery (Li et al., 2016b), molecular transporters (Shin and Pierce, 2004). Zhu et al. (2018a) designed

a pixel counting strategy based on DNzyme walker-triggered fluorescence spots for target DNA detection. DNzyme captured on glass slide were activated by target DNA and cut nearby fluorescein amidite-labeled hairpin substrates. The autonomous walking of this one-swing DNzyme walker initiated signal amplification. Chen's group (Cai et al., 2016) constructed DNzyme walker based electrochemical aptasensor for the detection of breast cancer cell. DNzyme released by target cell-responsive reaction, cleaved the substrates anchored on electrode into shorter strands, which produced decreasing electrochemical signal. Although the DNzyme walkers generate large amount of indicators in a single target binding event, the sensitivity of the DNzyme walker based sensors is intend for improve in trace analysis. DNA walkers.

Proximity ligation assay (PLA), a DNA-assisted immunoassay strategy, relies on the binding specificity of both antibodies and oligonucleotides (Koos et al., 2015). Two or more affinity probes simultaneously recognize the same target. Only binding of these probes are in the proximity of less than 40 nm, the hybridization of DNA labels were triggered to produce the detection signals that enables sensitive

* Corresponding author. Fax: +86 731-85258736

** Corresponding author.

E-mail addresses: jinglin_heCUST@hotmail.com (J.-L. He), zhongcao2004@163.com (Z. Cao).

<https://doi.org/10.1016/j.bios.2019.111692>

Received 18 July 2019; Received in revised form 1 September 2019; Accepted 6 September 2019

Available online 07 September 2019

0956-5663/© 2019 Elsevier B.V. All rights reserved.

detection of the target protein or oligonucleotides. In Ren's work (Ren et al., 2014), a target-induced proximity hybridization produced a triple-binder complex complementary with the DNA strand attached on mesoporous silica nanoprobe and thus opens the DNA biogate to release the electroactive methylene blue. Yuan's group (Peng et al., 2019) designed a target-driven DNA scissors for the proximity hybridization of microRNA-21 and following signal generation by the reversible switching of diethylenetriamine labeled DNA scissors to develop an electrochemiluminescence proximity assay. Therefore, proximity ligation assay has offered an alternative for selective recognition, which benefits from multiple binding events happened in a single target.

Human telomerase synthesizes new 5'-(TTAGGG)_n-3' repeats onto the ends of eukaryotic chromosomes (Blackburn, E.H., 2001). Activation of telomerase allows cells to overcome replicative senescence and maintain telomere stability during cell proliferation. A low level of telomerase is associated with telomere shortening and cellular senescence (Garcia et al., 2007). High telomerase activity is observed in over 85% of human tumor cell lines (Ahmed and Tollefsbol, 2003; Claudio et al., 2001). Thus telomerase is considered as an excellent molecular marker for the diagnosis of cancer. The identification of telomerase activity is crucial not only for early clinical tumor diagnosis but also for development of telomerase-targeted medicine (Lee et al., 2014; Ma et al., 2018). An well-established determination of human telomerase activity is the telomeric repeat amplification protocol (TRAP). The DNA substrate is extended by telomerase present in a crude cell lysate, and the resulting repeats are amplified by PCR (Kim et al., 1994). A variety of methods have been currently used to measure telomerase activity based on fluorescence (Zhu et al., 2018b), luminescence (Ma et al., 2017), surface plasmon resonance (Sharon et al., 2010), electrochemistry (Liu et al., 2015), surface enhanced Raman scattering and colorimetry (Zong et al., 2014). Among them, electrochemical detection draws our attention owing to the characteristic of low cost, high-sensitivity and the easy miniaturization.

Here we designed an electrochemical method that combines proximal binding with DNA walker for signal amplification. Telomerase extracted from HeLa cells recognized the primer and elongated with DNA sequence repeats, which hybridized with scaffold sequences to form DNAzyme spiders. The Cu²⁺-dependent DNAzyme cleaved and replaced substrates on surface and reattached nearby substrates. The released Fc-labeled fragments caused electrochemical signal amplification. DNAzyme spiders with three legs showed an excellent improvement in sensitivity over single molecule or two-component 'sandwich' binding. Our enzyme-free method was expected to expand the scope of DNA nanotechnology in the areas of clinical diagnosis.

2. Experimental section

2.1. Materials and reagents

All oligonucleotides, as illustrated in Scheme 1, were customer designed and synthesized by Sangon Inc. (Shanghai, China), and used as received, except when noted. DNAzyme-telomerase substrate primer (D-TSP) consisted of a Cu²⁺ specific DNAzyme (in green) and a telomerase substrate primer (in violet). Y1, Y2 and N1 probes were synthesized with Cu²⁺ specific DNAzyme at their 5'-terminus. The regions under dash line in the Y1, Y2 and N1 probes indicated complementary sequences to the synthetic telomerase products. The region under solid line in the Y1 probe was designed to hybridize with the underlined part of Y2 probe. Hairpin capture (HC) and T₁₂-hairpin capture (T₁₂-HC) were attached a mercapto group (SH) at the 5'-terminus and a ferrocene (Fc) at the 3'-terminus. The loops of HC and T₁₂-HC (in the blue bold typeface) were the substrate of Cu²⁺ specific DNAzyme, and their stem sequences were indicated as the italicized regions. All DNA probes were diluted in 50 mM HEPES buffer (pH 7.0) containing 1.5 M NaCl to give the stock solutions of 10 μM. The deoxynucleotide solution mixture (dNTPs) was purchased from Sangon Inc. (Shanghai, China) 4-(2-

hydroxyethyl)-1-piperazineethanesulfonic acid (HEPES), mercaptoethanol (MCH), phenylmethanesulfonyl fluoride (PMSF), 3-[(3-cholamidopropyl) dimethylammonio] -1-propanesulfonic acid (CHAPS), ethylene glycol bis (aminoethyl ether) -N,N,N',N'- tetraacetic acid (EGTA) were obtained from Sigma-Aldrich (St. Louis, MO, USA). Tris (hydroxymethyl) aminomethane (Tris), hydrochloric acid (HCl), NaCl, CuSO₄ and MgCl₂ were purchased from Sinopharm Chemical Reagent Co., Ltd. (Shanghai, China). All reagents were of analytical grade, and buffer solutions were prepared with ultrapure water (specific resistance of 18.25 MΩ cm⁻¹) that obtained from a laboratory ultrapure water system series (Kertone water treatment Co., Changsha, China).

2.2. Cell culture

HeLa (human cervical adenocarcinoma), MCF-7 (human breast adenocarcinoma) and A549 (human lung adenocarcinoma) were purchased from Cell Resource Center of Shanghai Institute for Biological Sciences (Chinese Academy of Sciences, Shanghai, China). HeLa cells and A549 cells were grown in RPMI-1640 medium (Corning). MCF-7 cells were maintained in Dulbecco's modified Eagle's medium (DMEM, GIBCO). All cells were incubated at 37 °C in a humidified atmosphere (95% air and 5% CO₂), and media were supplemented with 10% fetal bovine serum (Invitrogen).

2.3. Telomerase extracted from cells

The cells were counted using a Beckman cell counter and were collected in the exponential phase of growth. The about 10⁶ cells were transferred into a 15 mL EP tube and washed twice with ice-cold phosphate buffered saline (PBS) by centrifugation at 10000 rpm for 3 min at 4 °C. Then the cells were resuspended in 100 μL of ice-cold CHAPS lysis buffer (0.5% CHAPS, 10 mM Tris-HCl, pH 7.5, 1 mM MgCl₂, 1 mM EGTA, 0.1 mM PMSF, 5 mM mercaptoethanol, 10% glycerol). The lysate was incubated in an ice bath for 30 min and centrifuged at 12000 rpm for 20 min at 4 °C. The resulting extract was used immediately for the telomerase extension reactions. In the control experiment, the telomerase extract was treated at 95 °C for 10 min.

2.4. Telomerase extension reactions

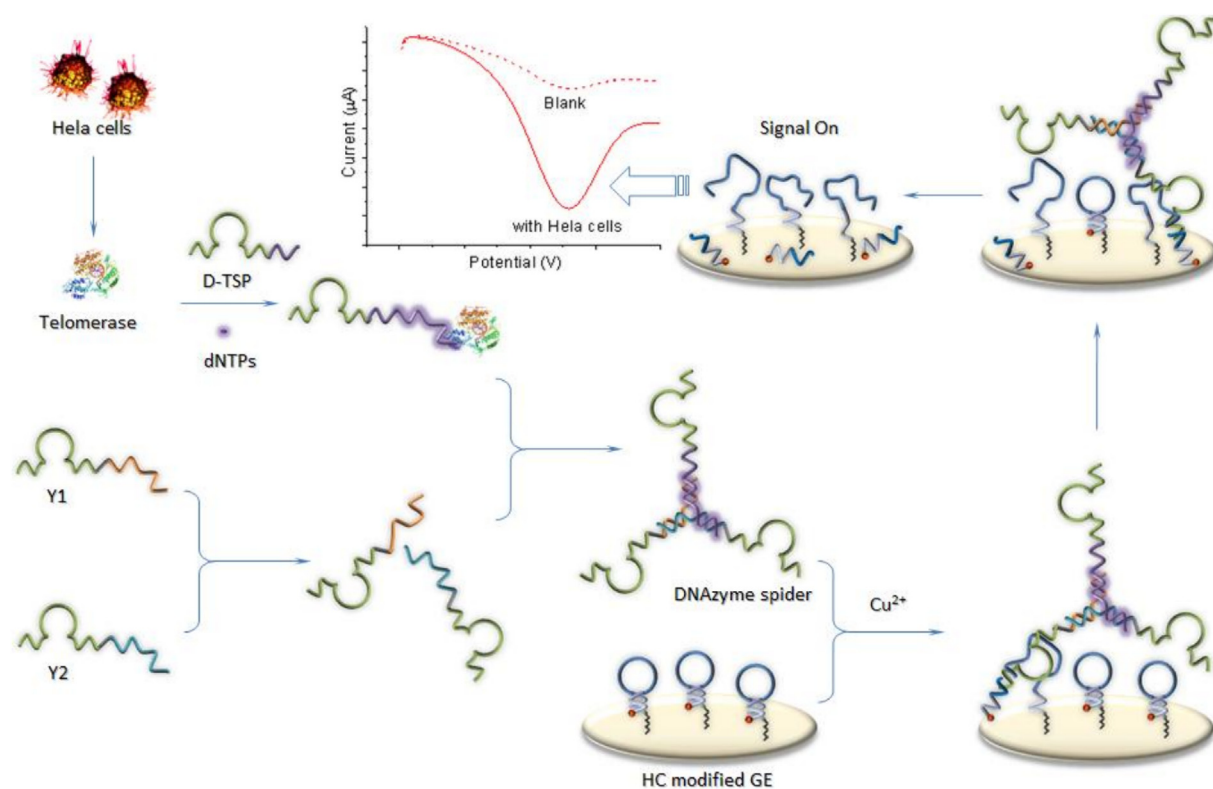
For telomerase extension reactions, 5 μL of the telomerase extracts equivalent to a series of respective number of cells were added to 45 μL of extension solution containing D-TSP (0.5 μM), dNTP (1 mM), RNase inhibitor, and reaction buffer (20 mM Tris-HCl, pH 8.3, 1.5 mM MgCl₂, 63 mM KCl, 1 mM EGTA, 0.005% Tween 20, and 0.1 mg/mL BSA). The result solution was incubated at 37 °C for 90 min, and then heated to 94 °C for 10 min to end the reaction. The synthetic telomerase products were obtained to synthesize DNAzyme spiders.

2.5. Synthesis of DNAzyme spiders and sensing procedure

The DNAzyme spider was prepared with a final Y1 probes concentration of 2.5 nM and a Y2 probes concentration of 2.5 nM in 50 mM HEPES buffer (pH 7.0) containing 1.5 M NaCl. Then 10 μL of synthetic telomerase products was added to the resultant mixture, and incubated for 20 min to form the DNAzyme spider.

The gold electrodes (GE) were polished with Al₂O₃ slurries (0.3 and 0.05 μm) on chamois pads. Trace alumina was removed by sonication in deionized water and ethanol. After treated in piranha solution (H₂SO₄: H₂O₂ = 7:3) for 20 min, the GEs were electrochemically cleaned in 0.10 M H₂SO₄ solution by cyclic potential scanning between 0 and 1.7 V till a standard CV was obtained. 10 μL of 2.0 μM HC probes was cast on the treated GE, and incubated overnight at 4 °C.

DNAzyme spider was incubated on the HC probes modified GE for 30 min. Cyclic voltammetry (CV) and square wave voltammetry (SWV) measurements were performed using a CHI 660E electrochemical



Scheme 1. Schematic illustration of the telomerase-triggered synthesis of DNAzyme spiders that spontaneously migrates across a capture probe modified electrode and its application for a sensitive electrochemical assay. Green lines: a DNAzyme strand; Purple lines: a telomerase substrate primer; Purple lines highlighted: telomerase products; Blue lines: a substrate; Red dot: Fc.

analyzer (Shanghai Chenhua Equipments, China). SWVs were registered in the potential interval 0 to +0.40 V. CV were recorded at scan rates of 40–220 mV s⁻¹ and were let run for at least six full cycles. The electrochemical system consisted of gold working electrode, a platinum wire counter electrodes, and Ag–AgCl reference electrodes. All potentials were referenced to the Ag–AgCl reference electrodes.

Polyacrylamide gel electrophoresis (PAGE, Junyi, Beijing, China) was performed on a 15% denatured gel. The running buffer was 1 × TBE (pH 8.0, Dingguo, China) containing 89 mM Tris-HCl, 89 mM boric acid, and 2 mM EDTA (Sinopharm). The gels were stained using 100 × SYBR Gold (Thermo Fisher Scientific) to image the position of DNA. The gel was run at 120 V for 130 min after introduction of the samples. Photographic images were obtained under visible light with a gel documentation and image analysis system (Sagecreation, Beijing, China).

3. Results and discussion

3.1. Principle of the telomerase-triggered DNAzyme spiders based assay

The principle of the exponential amplified electrochemical assay integrates synthesis of telomerase-triggered DNAzyme spiders and a strand-displacement strategy (Scheme 1). Telomerase extracted from HeLa cells recognizes the primer and elongate D-TSP with DNA sequence repeats (“TTAGGG”) at the 3′-terminus. The generated telomerase products hybridize with scaffold sequences of Y1 (in orange) and Y2 (in blue) probes to form DNAzyme spiders with three catalytic legs. These legs are adapted from the DNAzyme, which contains a catalytic core and two recognition regions that bind to a DNA substrate through Watson-Crick base-pairing. With the assist from Cu²⁺, DNAzyme cleaves HC substrates on GE surface into two fragments, which dissociate from the DNAzyme. Then the recognition regions of the DNAzyme become active to reattach another nearby HC substrate. As a

result, a strand displacement occurs through branch migration, and DNAzyme spiders move from one site to an accessible neighbouring site until it finds another substrate to bind, cleave and replace. A large amount of released Fc-labeled fragments left on GE surface and lead to considerable electrochemical signal amplification eventually. In the blank experiment, D-TSP keeps its short strand with low affinity to form DNA machines. Single DNAzyme cleaves HC and completely dissociates, but it will not quickly reattach to a nearby substrate site. In consequence, weak signals are produced from a few of Fc-labeled cleaved fragments.

3.2. Feasibility of the DNAzyme spiders based strategy for cancer cell assay

The feasibility of the target-triggered DNAzyme spiders based strategy was investigated by CV and SWV to confirm the detection of telomerase using Fc as a redox indicator. As shown in Fig. 1, the CV of control experiments did not show any detectable signal in PBS (curve a). When the proposed sensor is incubated with synthetic telomerase products, a pair of stable redox peaks was observed at -0.178 and -0.268 V (curve a'), which correspond to the electrochemical response of Fc.

The anodic peaks (I_{pa}) of Fc molecule on the modified electrode were used to reflect the surface chemistry. As shown in Fig. 2, the SWV curve was almost unchanged on bare GE surface (curve a). The SWV response slightly increased on HC modified GE (curve b). It means Fc labeled HC strands were covalent attached on GE and form hairpin conformation as expected. The Y1 or Y2 probe contains a DNAzyme leg and a hybridization arm that can partly bind to a synthetic telomerase product extracted from HeLa cells. We attempted to explore the electrochemical responses by individually employing Y1 (curve c and c') or Y2 (curve d and d'), in order to verify that the electrochemical response was indeed aroused by the close proximity of two sequences of Y1 and Y2 at the 3′-terminus after telomerase reaction. No evident

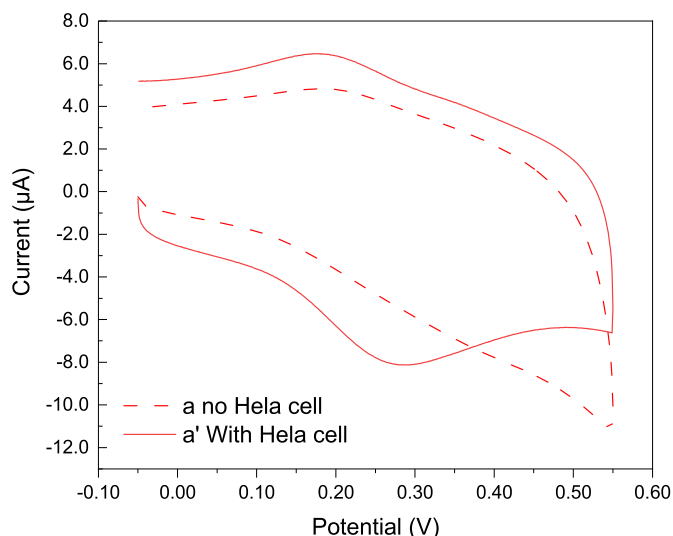


Fig. 1. CV of telomerase-triggered DNAzyme spiders incubated on HC-GE with (solid line) or without (dashed line) 2000 HeLa cells in the 10 mM PBS (pH 7.4) containing 2.7 mM of KCl and 137 mM of NaCl.

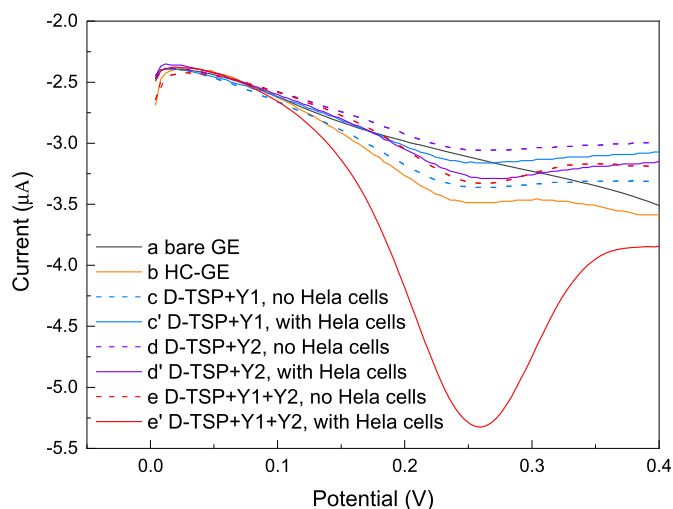


Fig. 2. SWV of different DNAzyme walkers incubating on electrode interface. Bare GE(a), HC modified GE(b), D-TSP + Y1 without (c) or with (c') telomerase, D-TSP + Y2 without (d) or with (d') telomerase, D-TSP + Y1+Y2 without (e) or with (e') telomerase, respectively. The telomerase extracted from 2000 HeLa cells.

electrochemical responses were obtained after telomerase incubation, which strongly verified the proximity-based hybridization was suspended and DNA walkers were not formed yet. The incubation of the sensing surface with the mixture of D-TSP, Y1 and Y2 only causes negligible changes in the current responses (curve e). It seems that the lack of synthetic telomerase products leads to the low efficiency of cleavage of HC probes and the dissociation of the cleaved fragments. A significant increase in anodic peak current is obtained (curve e') after the assembly of the synthetic telomerase product-containing ternary complex and incubation on HC modified GE. Telomerase prolonged D-TSP with "TTAGGG" sequence repeats, and initiated proximity-based assembly of DNAzyme spiders that comprised a "Y" shape inert body and three catalytic legs. These DNAzyme legs binded the substrates on GE, and caused enzymatic cleavage of the Fc-labeled sequences and the stepwise movement of the spiders along the surface tracks.

3.3. X-ray photoelectron spectroscopy (XPS) analysis

The changes in surface chemistry have been proven by XPS analysis as shown in Fig. S1. The characteristic peak of Au4f at about 83.63 eV was observed on the bare Au plate (curve a). A significantly decreased signal was appeared in this peak on HC modified Au (b), owing to surface coverage. The typical peaks of S2p and N1s located at about 168.1 eV and 399.3 eV were attributed to thiol tethered DNA appeared at Au plate, indicating the successful self assembly of HC on Au surface. The photoelectron signal for C1s (285.3 eV) was slightly enhanced on HC modified Au incubating with DNAzyme spiders (curve c), which indicated that the Au surface was more densely packed with DNA probes. After addition of Cu^{2+} , the O1s binding energy at 531.5 eV was increase, while further decrease was observed at the peaks of Au 4f. The data reveals that DNAzyme catalyzes oxidative self-cleavage with assistance of Cu^{2+} , and the cleaved fragment even covered the Au plate. The XPS result further confirmed the successful attachment of HC probes to the Au surface and effective cleavage induced by DNAzyme spiders.

3.4. Electrochemical impedance spectroscopy (EIS) characteristics

HC-1 probe without Fc (5'-HS-CGAT CCAA AGCT TCTT TCTA ATAC GGCT TACC TTGG ATCG) was utilized in EIS to characterize the biosensor surface, using $[\text{Fe}(\text{CN})_6]^{4-/3-}$ couple as a redox probe in the PBS solution. Fig. S2 illustrated the Nyquist plots obtained at different fabrication stages of GE. Equivalent circuit for the electrochemical cell was shown in the inset. In all these plots, the diameter of the semicircle represented the electron transfer resistance (R_{et}) at the GE surface. The bare GE exhibited very small semicircle (233.5 Ω) at high frequencies (curve a). The R_{et} increased remarkably to 3463 Ω after self-assembling of HC-1 on the electrode (curve b). This was attributed to the fact that the HC-1 assembling on the GE generated an insulating layer and prohibited the transfer of redox couple $[\text{Fe}(\text{CN})_6]^{3-/4-}$ to the surface. After the incubation of the mixture of Y1 and Y2 (curve c), obvious decrease ($R_{\text{et}} = 2770 \Omega$) was observed. It revealed that hybridization between DNAzyme and HC probes played a role similar to an adjacent helical conduction path to improve the electron transfer (Huang et al., 2008). The R_{et} further decreased to 2115 Ω after incubation of DNAzyme spider on the HC modified GE (curve d), owing to more double-helical DNA conduction path formed by HC probes and DNAzyme spiders. An increase of R_{et} to 2481 Ω (curve e) was observed after DNAzyme spiders incubation and Cu^{2+} assistant cleavage. The cleaved fragment covered on GE caused electrostatic repulsion between DNA phosphate backbone and the negatively charged $[\text{Fe}(\text{CN})_6]^{3-/4-}$. The EIS results indicated that the process of modification, hybridization and cleavage were successfully accomplished on the GE surface.

3.5. Polyacrylamide gel electrophoresis assay

The PAGE gel electrophoresis experiment was performed to verify the target-fueled recycling process (Fig. 3). Y1 (Lane 1), Y2 (Lane 2), D-TSP (Lane 3) was observed according to the appearance of short-fragment bands. In the presence of normal HeLa cells extract, a new band with low mobility was obtained (Lane 4), which could be attributed to the long DNA strands triggered by telomerase. HC probes (Lane 5, $1.5 \mu\text{mol L}^{-1}$) ran as no bands due to their single strands. Lane 6 contained the complexes of Y1, Y2 and synthetic telomerase products. A bright and wide band with obviously decreased migration shift was observed (Lane 6), while the band of Y1 or Y2 was disappeared. This phenomenon indicated the formation of three-strand DNAzyme spiders by the strands of Y1, Y2 and synthetic telomerase products. The movement of the DNAzyme spiders was demonstrated by monitoring the differential cleavage behaviors of the HC substrate. There were clear short strand bands observed for the control experiment (Lane7) where the three strand assembly hybrids and substrate cleavage could

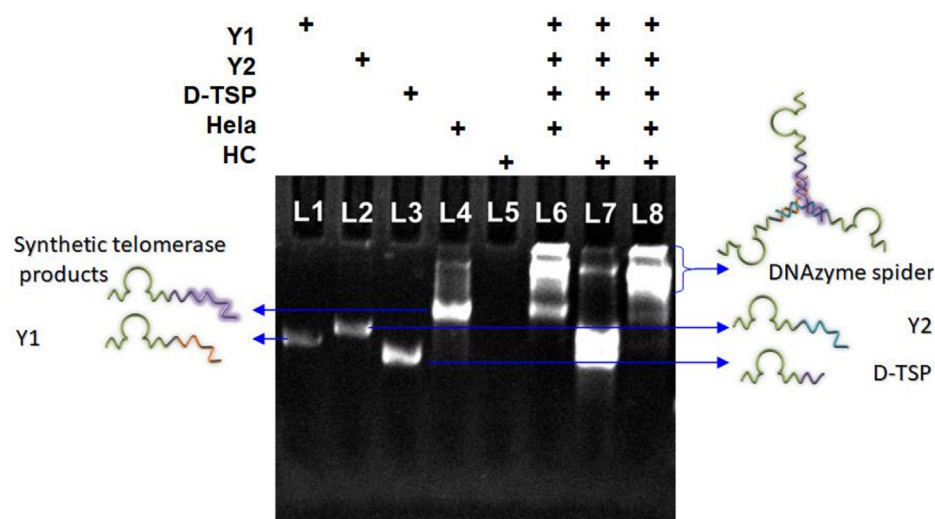


Fig. 3. The image of the PAGE gel electrophoresis samples captured under ultraviolet light. Lane 1: Y1; Lane 2: Y2; Lane 3: D-TSP; Lane 4 contained synthetic telomerase products; Lane 5 HC; Lane 6 contained Y1, Y2 and synthetic telomerase products; Lane 7 contained Y1, Y2, D-TSP and HC probes; Lane 8 contained Y1, Y2, synthetic telomerase products and HC probes. The telomerase extracted from 2000 HeLa cells.

not be triggered without the telomerase. In the presence of HeLa cells extract (Lane 8), the desired product-DNAzyme spiders exhibited extremely low mobility, suggesting the high molecular weight of the Y-shaped junction structure products. Single strand bands were not appeared, verifying the recycling cleavage process for the association of telomerase. These results clearly demonstrated that target-triggered DNAzyme spiders based strategy can be utilized for enormous signal amplification in bioanalysis.

3.6. Optimization of experimental condition on the response of the proposed sensor

In order to improve the analysis and compare migration dynamics of DNA machine with bulk strand displacement reactions, the N-shape DNAzyme walker and Y-shape DNAzyme spider were tested on HC tethered electrodes, as shown in Fig. S3. After incubation with heated HeLa cells, negligible SWV responses were exhibited in N-shape DNAzyme walker system (curve a) and Y-shape DNAzyme spider system (curve b). Few of stable DNA machine were formed because of the short strands of D-TSPs. N1 probes and partial complementary Y1/Y2 duplex display low cleavage and migration efficiency. In the presence of HeLa cells, N-shape DNAzyme walker system shows observable response (curve a'). D-TSPs were prolonged with repeatable sequences by active telomerase. N1 strands hybridize with synthetic telomerase products into a complementary, N-shaped duplex, which enables activation of substrate cleavage on surface. A noticeable anodic peak is observed in Y-shape DNAzyme spider based analysis (curve b'). Although the partial complementarity of the Y1 and Y2 strands is insufficient to form a stable duplex, the addition of synthetic telomerase products results in hybridization into a stabilized ternary Y-shape complex that allows for well migration. As a result, a large amount of cleaved Fc-labeled fragments gathered on electrode produced higher peak current, which is required for optimal DNA machine design and application.

Fig. S4 presents a bar chart of the anodic peak current signal (at 0.264 V) as a function of the telomerase reaction time (0, 30, 60, 90, 120, and 150 min). It is clear that the current signal of the sample increases significantly with the telomerase reaction time. When the telomerase extracted from HeLa cells was introduced, remarkable peak current was observed in the first 90 min. SWV response stopped obvious increasing and tended to be steady after 90 min. This was attributed to the tendency of D-TSP extension to cease because of exhaustion of the various materials as the reaction time exceeded 90 min. As a result, 90 min was selected for the primer extension time. These results show that the DNAzyme spider formation and migration was successfully triggered by telomerase extension.

Stem sequences of the surface-tethered probes was predicted to facilitate the conformational change that led to Fc release to the electrode, and result in an increase in SWV responses. In Fig. S5, three different thiolated hairpin probes that were substrate to the Cu^{2+} specific DNAzyme were utilized: HC-T12 probes, HC-T12/A12 duplexes and HC probes. HC-T12 probe contained T12 spacer as a tail sequence. The A12 strand can be hybridized with complementary T12 spacer and result in 19-bp stem of HC-T12/A12 duplexes. The low level of SWV signal from the negative control (curve a, curve b and curve c) indicates a negligible substrate cleavage and Fc-fragment adsorption onto the electrode surface. In the presence of active HeLa cells, HC modified GE (curve c') achieved the better signal to background ratio than that on HC-T12 (curve a') or HC-T12/A12 duplexes (curve b') modified GEs. It suggested that neither the tail sequences in HC-T12 nor the scaffold strands in HC-T12/A12 duplexes facilitate substrate cleavage and Fc aggregation. HC is indeed an important elements contributed to the successful solid-phase strand-displacement and signal amplification.

As displayed in Fig. S6, the unblocked HC-GC gives a well-defined SWV peak (curve a) because of the good electrical conductivity of Fc molecule labeled on HC. When the telomerase was introduced to form DNAzyme spiders, dramatic increase in positive currents was observed (curve a'). It revealed that DNAzyme spiders initiate the recycling DNA substrate cleavage, and the cleaved products showed enhanced accessibility to the electrode interface. A subsequent surface blocking with MCH causes an obvious decrease in the current responses (curve b and b'), and no peak separation can be observed owing to the repulsion of Fc-segments from approaching the electrode interface by the MCH, and force the Fc labeled complexes to orientate towards the electrolyte solution. Therefore, the unblocked HC-GCs were used in following experiments.

The effect of scan rate on the peak current was investigated to study the controlled factor of the electrochemical process on the electrode surface. At scan rates in the range from 0.040 to 0.220 V/s, the oxidative and reduction peak currents of the proposed sensor (Fig. S7A) in the presence of HeLa cells increase with the scan rate. Fig. S7B shows the linear relationship between the peak currents and scan rates, with the equation, $I_{pa} (\mu\text{A}) = -0.4211 - 5.302 \text{ Scan rate (V/s)}$ (with correlation coefficient $r = 0.9989$), which confirmed that the process is controlled by the surface reaction, and the Fc-conjugated fragments are adsorbed to the electrode surface. The interface properties of the electrode illustrated signal enhancement were indeed caused by the cleavage of the DNAzyme spiders.

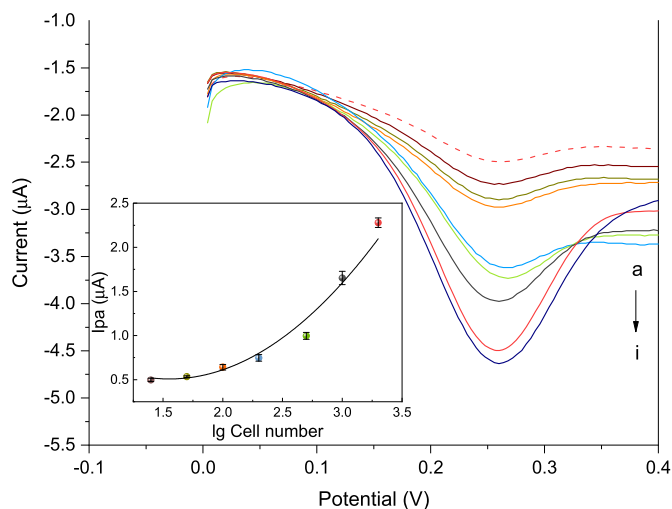


Fig. 4. SWV of telomerase-triggered DNzyme spiders for electrochemical assay of HeLa cells at a series of cell numbers. From top to bottom: 0, 25, 50, 100, 200, 500, 1000, 2000, and 4000 cells. Inset: The calibration Plot of logarithm HeLa cell numbers (25–2000) vs peak current (error bars: SD, $n = 3$).

3.7. Sensitivity for the detection of telomerase activity

According to the optimized conditions above, the telomerase-triggered DNzyme spiders based exponential amplified assay was carried out to detect HeLa cells, as shown in Fig. 4. Well defined SWV responses were observed at about 0.26 V for a series of HeLa cell numbers. The SWV had nearly the same peak position and shape with that of the standard solution of HeLa cells, indicating the SWV signals was ascribed to telomerase extracted from HeLa cells. The current responses of products increased dramatically with the increase of HeLa cell numbers from 25 to 4000. The responses were saturated at cell numbers beyond 4000. The inset shows a good nonlinear correlation ($R^2 = 0.9938$) between peak currents and the logarithm of the HeLa cell numbers, with the improved dynamic range from 25 to 2000 HeLa cells. The regression equation was $I_{pa} (\mu A) = 0.5194 \times (\lg \text{Cell number})^2 - 1.812 \times (\lg \text{Cell number}) + 1.760$. A detection limit of 16 cells was determined from three times the standard deviation of the baseline rate. The sensitivity of our work is comparable to or even better than that of the previously reported assays for telomerase activity (Table S1). The nonlinear behavior was due to the dendritic pattern of the amplification route rather than one-to-one or two-component ‘sandwich’ binding model. Telomerase arouse multiple DNzyme spider assembly, and then induced several strand displacement recycles, which resulted in an efficient increase of the effective SWV signals.

3.8. Selectivity for the detection of telomerase activity

To ensure the selectivity, we evaluated several kinds of cell lines (HeLa, A549, MCF-7) using the proposed method (Fig. 5). It was clearly that three cell lines had diacritical telomerase activity, whereas the heat-treated HeLa cells showed a weak signal used as control. These results revealed the reliability of this strategy for the detection of telomerase activity.

4. Conclusions

In summary, an electrochemical strategy combined DNA walker with proximity ligation assay is successfully demonstrated for the analysis of telomerase. The changes on surface of the target-triggered DNzyme spiders based biosensor was investigated by XPS and EIS to confirm the detection of telomerase using Fc as a redox indicator. This approach has the advantage that the proximity ligation assay

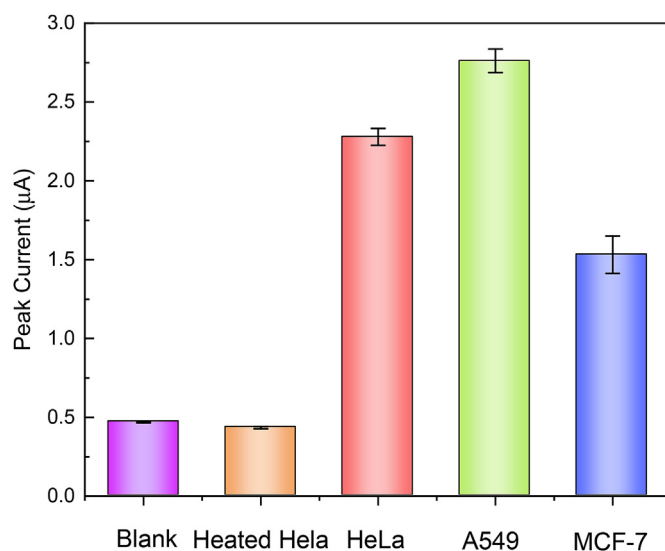


Fig. 5. SWV response for quantifying telomerase activity extracted from PBS (blank), heated HeLa, normal HeLa, A549, MCF-7 cell lines (2000 cells).

simultaneous synthetic telomerase products hybridization of a pair of affinity probes, facilitating the formation of DNzyme spiders. This strategy not only greatly enhances the stability of DNA walker but also improves the dynamic range of detection. Meanwhile, three-legs DNzyme spiders quickly explore sites nearby until they find another intact substrate to reattach to and cleave after cleaving one substrate, thus leading to considerable signal amplification eventually. In addition, the proposed sensor also accurately evaluated activities of telomerase that isolated from different cell lines. The method reported here was sensitive, enzyme-free, PCR-free, simple in operation which indicated that it is a robust promising research platform for measuring tumor biomarkers and clinical diagnostics.

CRediT authorship contribution statement

Jing-Lin He: Writing - review & editing, Conceptualization, Methodology, Supervision. **Yang Zhang:** Data curation, Writing - original draft. **Ting-Ting Mei:** Data curation, Investigation, Software. **Ling Tang:** Data curation, Software, Validation. **Si-Ying Huang:** Software, Validation. **Zhong Cao:** Supervision.

Declaration of competing interest

The authors declare that they have no known competing financial interests or personal relationships that could have appeared to influence the work reported in this paper.

Acknowledgments

This work was financially supported by the projects of National Natural Science Foundation of China (Nos. 21645009, 31527803, 21545010), Natural Science Foundation of Hunan Province (No. 2018JJ2419) and STS Program of the Chinese Academy of Sciences (No. KFJ-SW-STS-173).

Appendix A. Supplementary data

Supplementary data to this article can be found online at <https://doi.org/10.1016/j.bios.2019.111692>.

References

- Kim, N.W., Piatyszczek, M.A., Prowse, K.R., Harley, C.B., West, M.D., Ho, P.L., Coviello, G.M., Wright, W.E., Weinrich, S.L., Shay, J.W., 1994. *Science* 266, 2011–2015.
- Ahmed, A., Tollefsbol, T., 2003. *J. Am. Geriatr. Soc.* 51, 116–122.
- Blackburn, E.H., 2001. *Cell* 106, 661–673.
- Cai, S., Chen, M., Liu, M., He, W., Liu, Z., Wu, D., Xia, Y., Yang, H., Chen, J., 2016. *Biosens. Bioelectron.* 85, 184–189.
- Claudio, O., Stefania, G., Cesare, S., Mario, P., 2001. *J. Urol.* 166, 666–673.
- García, C.K., Wright, W.E., Shay, J.W., 2007. *Nucleic Acids Res.* 35, 7406–7416.
- He, M., Wang, K., Wang, W., Yu, Y., Wang, J., 2017. *Anal. Chem.* 89, 9292–9298.
- Huang, Y.C., Ge, B., Sen, D., Yu, H.-Z., 2008. *J. Am. Chem. Soc.* 130, 8023–8029.
- Koos, B., Cane1, G., Grannas, K., Löf, L., Arngården, L., Heldin, J., Claesson, C.-M., Klaesson, A., Hirvonen, M.K., de Oliveira, F.M.S., Talibov, V.O., Pham, N.T., Auer, M., Danielson, U.H., Haybaeck, J., Kamali-Moghaddam, M., Söderberg, O., 2015. *Nat. Commun.* 6, 7294–7303.
- Lee, M., Hills, M., Conomos, D., Stutz, M.D., Dagg, R.A., Lau, L.M.S., Reddel, R.R., Pickett, H.A., 2014. *Nucleic Acids Res.* 42, 1733–1746.
- Li, D., Cheng, W., Li, Y., Xu, Y.J., Li, X., Yin, Y., Ju, H., Ding, S., 2016a. *Anal. Chem.* 88, 7500–7506.
- Li, F., Cha, T., Pan, J., Ozcelikkale, A., Han, B., Choi, J.H., 2016b. *Chembiochem* 17, 1138–1141.
- Li, P., Wei, M., Zhang, F., Su, J., Wei, W., Zhang, Y., Liu, S., 2018. *ACS Appl. Mater. Interfaces* 10, 43405–43410.
- Liu, X., Li, W., Hou, T., Dong, S., Yu, G., Li, F., 2015. *Anal. Chem.* 87, 4030–4036.
- Lund, K., Manzo, A.J., Dabby, N., Michelotti, N., Johnson-Buck, A., Nangreave, J., Taylor, S., Pei, R., Stojanovic, M.N., Walter, N.G., Winfree, E., Yan, H., 2010. *Nature* 465, 206–210.
- Ma, W., Fu, P., Sun, M., Xu, L., Kuang, H., Xu, C., 2017. *J. Am. Chem. Soc.* 139, 11752–11759.
- Ma, Y., Wang, Z., Ma, Y., Han, Z., Zhang, M., Chen, H., Gu, Y., 2018. *Angew. Chem. Int. Ed.* 57, 5389–5393.
- Nie, Y., Zhang, P., Wang, H., Zhuo, Y., Chai, Y., Yuan, R., 2017. *Anal. Chem.* 89, 12821–12827.
- Peng, L., Yuan, Y., Fu, X., Fu, A., Zhang, P., Chai, Y., Gan, X., Yuan, R., 2019. *Anal. Chem.* 91, 3239–3245.
- Qing, M., Xie, S., Cai, W., Tang, D., Tang, Y., Zhang, J., Yuan, R., 2018. *Anal. Chem.* 90, 11439–11445.
- Ren, K., Wu, J., Zhang, Y., Yan, F., Ju, H., 2014. *Anal. Chem.* 86, 7494–7499.
- Sharon, E., Freeman, R., Riskin, M., Gil, N., Tzfati, Y., Willner, I., 2010. *Anal. Chem.* 82, 8390–8397.
- Shin, J.-S., Pierce, N.A., 2004. *J. Am. Chem. Soc.* 126, 10834–10835.
- Tomov, T.E., Tsukanov, R., Liber, M., Masoud, R., Plavner, N., Nir, E., 2013. *J. Am. Chem. Soc.* 135, 11935–11941.
- Wang, D., Vietz, C., Schröder, T., Acuna, G., Lalkens, B., Tinnefeld, P., 2017. *Nano Lett.* 9, 5368–5374.
- Wang, J., Wang, D., Tang, A., Kong, D., 2019. *Anal. Chem.* 91, 5244–5251.
- Xu, Z., Liao, L., Chai, Y., Wang, H., Yuan, R., 2017. *Anal. Chem.* 89, 8282–8287.
- Yan, T., Zhu, L., Ju, H., Lei, J., 2018. *Anal. Chem.* 90, 14493–14499.
- Zhang, D.Y., Winfree, E., 2009. *J. Am. Chem. Soc.* 131, 17303–17314.
- Zhang, P., Li, Z., Wang, H., Zhuo, Y., Yuan, R., Chai, Y., 2017. *Nanoscale* 9, 2310–2316.
- Zhu, L., Liu, Q., Yang, B., Ju, H., Lei, J., 2018a. *Anal. Chem.* 90, 6357–6361.
- Zhu, X., Ye, H., Liu, J.-W., Yu, R.-Q., Jiang, J.-H., 2018b. *Anal. Chem.* 90, 13188–13192.
- Zong, S., Wang, Z., Chen, H., Hu, G., Liu, M., Chen, P., Cui, Y., 2014. *Nanoscale* 6, 1808–1816.